Interference-aware Joint Optimization in Rechargeable Wireless Sensor Networks

Yi Qu*, Ke Xu*, Haiyang Wang†, Meng Shen§, and Bo Wu*

*Computer Science and Technology, Tsinghua University, China
†Computer Science, University of Minnesota at Duluth, USA
§Computer Science and Technology, Beijing Institute of Technology, China
Email:{quy11@mails, xuke@mail, wub14@mails}.tsinghua.edu.cn,
haiyang@d.umn.edu, shenmeng@bit.edu.cn

Abstract. Radio Frequency based Wireless Power Transfer (RF-WPT) technology is recognized as a promising way to charge low-power wireless devices. But the application of RF-WPT in wireless sensor networks also introduces charging interference to wireless communications. The network performance optimization by jointly considering wireless charging and data transmission under interference concerns, however, has seldom been examined. In this paper, we study the data communication and charger scheduling together in rechargeable wireless sensor networks. We propose a smart interference-aware scheduling to maximize the network profit and avoid potential data loss caused by charging interference. Then, we theoretically prove the optimality, lower and upper bound of the proposed design. The evaluation result indicates that the proposed design can guarantee 99% optimality and significantly improve network lifetime.

Keywords: Wireless sensor network, Power transfer, optimization

1 Introduction

There has been an increasing research interest over the past few years in Radio Frequency based Wireless Power Transfer(RF-WPT) [5][9][15]. In this design, the ambient RF radiation can be captured by the receiver antennas and converted into electrical energy. Comparing to the traditional magnetic resonant coupling approaches [10], RF-WPT is known as a suitable way to wirelessly charge such ultra-low power devices as sensors and RFIDs [11][22]. However, the radiation of RF signal also introduces severe interference to the wireless communication. In particular, sensors will experience 100% data loss when a RF generator is operating within 140 meters with 1Watt Energy Transmission(ET) power, which brings significant challenges to the real-world RF-WPT deployment [14].

In this paper, we for the first time investigate this charging interference in the joint optimization of RF-WPT charging and data routing in WSNs. Our model carefully captures the charging as well as the routing behaviors in RF-WPT system, aiming to provide a smart coordination between charger movement and data

routing. Similar to the existing studies [16][17][21], we also aim to maximize the network profit in WSNs to better balance the network lifetime and charging cost. Unfortunately, our model analysis indicates that the joint optimization is NP-hard due to the existence of charging path planning sub-problem. To address this challenge, we carefully explore a set of possible approximations step by step. As shown in Fig. 1, we start with an approximation to relax the energy constraints. In detail, this allows sensors to be temporarily out of power and transforms the original problem(OR) into an upper-bound problem(UP). We prove that the relaxation can successfully decouple the dependency between network lifetime and the charger's traveling path, making the upper-bound problem solvable in polynomial time. Based on the investigation of the upper-bound problem, we further construct a near-optimal problem(NR) where the out-of-power relaxation is removed by assigning extra energy to sensors in the initialization stage. Moreover, a lower-bound problem(LOW) is also examined to bound the approximate ratio of NR. According to the above model analyses, we finally propose a near-optimal solution to address the joint optimization problem. The evaluation shows that our solution achieves 90% approximate ratio in different network environments and significantly prolongs the network lifetime. The main contributions of this paper include:

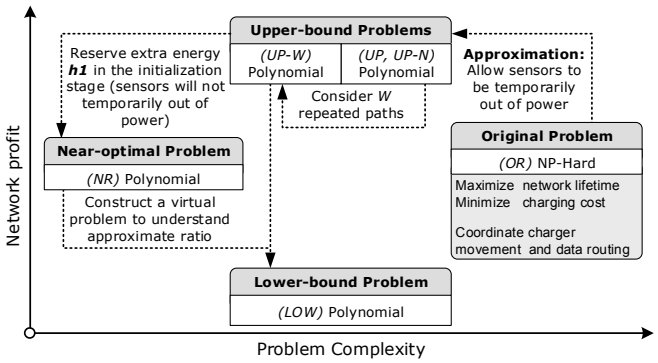

Fig. 1. Problems discussed in this paper.

- We pinpoint the key challenge in such joint optimization and provide well-designed relaxations to simplify the problem. The proposed approximations can also be applied to better understand other energy-related issues in WSNs.
- We develop a near-optimal solution to the original problem; the approximate ratio is also bounded based on the analysis of upper-bound and lower-bound problems.

The rest of this paper is organized as follows: In Section 2, we present the related work. Section 3 describes the big picture of our system model and de-

fines the problem. Section 4 and 5 discuss the modeling of charging and routing behaviors, respectively. Based on the charging and routing constraints, Section 6 considers the balancing of network lifetime as well as charging cost. The joint optimization problem is then proposed and relaxed in section 7. Section 8 solves the joint optimization with bounded approximate ratio. This solution is then extensively evaluated in Section 9. Section 10 concludes the paper.

2 Related Work

WSN lifetime maximization as well as its energy efficiency have been tackled in the scientific literature from many aspects. One of the earlier work is GAF(Geographical Adaptive Fidelity) [25], which divided network area into virtual grids. In each grid, only one sensor is required to be active to communicate, and others stay in sleep state to reserve energy. To better consider the data forwarding costs, Bandyopadhyay *et al.* [2] proposed an energy-efficient distributed routing. This approach organizes sensors into a hierarchy of clusters, where sensors only communicate to cluster-heads and then the cluster-heads forward the aggregated data to the sink. Recently, mobile sink [12], relay [29] and data collector [18] have also been extensively considered as alternative solutions to energy-efficient data collection in WSNs.

Breakthrough in WPT technology offers a new option to dynamically recharge energy-scarce sensors. Kurs *et al.* [10] experimentally showed that, by exploiting magnetic resonant coupling, wireless power transfer is feasible and practical. Realizing the enormous potential of WPT, a flourish of research efforts were paid to apply WPT in WSNs [20][24][6][7][4][3][28]. In particular, Shi *et al.* [20] investigated a mobile wireless charging vehicle(WCV), and the sensor batteries were replenished in a periodical manner. When adopted in WSNs, this design can make sensors stay operational forever. To understand the efficiency of WCV, the mathematical analysis from Xie *et al.* [24] proved that bundling the base station on the WCV could further promote network performance. Based on this observation, Guo *et al.* [6] considered an anchor-point based mobile data gathering scheme and aimed to maximize total network utility. He *et al.* [7] and Zhang *et al.* [28] indicated that the charger location as well as its deployment will also affect the charging efficiency. Fu *et al.* [4] further considered the charger location and studied the minimum charging delay problem. A recent study from Dai *et al.* [3] also attempted to transfer maximum power under a predefined electromagnetic radiation threshold.

Different from traditional WPT, the Radio frequency based technique, RF-WPT, utilizes wireless power carried by radio frequency signals. In 2008, Sample *et al.* [19] designed a RF-WPT system that consists of a RF signal generator and a WISP(Wireless Identification Sensing Platform) node. This system can collect RF signal and rectify it to electric currents. Comparing to magnetic resonant coupling, RF-WPT is recognized as the most suitable way to charge devices with ultra-low power requirements such as sensors and RFIDs [11] [22]. This is due to the simplicity of RF-WPT deployment. In particular, it can be imple-

mented by adding such basic electronic elements as rectifiers, capacitors and diodes to the existing circuits. The deployment overheads of large coils(with diameter of 0.6m in magnetic resonant coupling [10]) and scrupulous resonance alignments are therefore greatly minimized.

Although RF-WPT is a good match for sensor networks, it introduces charging interferences to the wireless data communication [13]. This is because the RF signals exhibit higher signal strength than the low-power data communications [11]. In general, severe data loss will be experienced whenever the power transfer and the data communication happen simultaneously. For example, Naderi *et al.* [14] has reported that sensors will experience 100% data loss when a RF generator is operating within 140 meters with 1Watt ET power. However, how to consider such an interference is not yet examined in the existing wireless routing frameworks.

3 System Model and Problem Definition

Let N be the finite set of wireless sensors, distributed randomly in a two-dimensional area. Each sensor can be recharged by RF signal and has initial battery power h_0. To monitor the interested area, each sensor $i \in N$ generates sensory data with the rate of g_i, and the data will be forwarded to the sink through multi-hop wireless communications. To charge these sensors, a mobile RF charger starts off from the sink and visits the sensors within the area. We use L to denote the sensor sequence which the charger will visit. Since the charger can visit a sensor for multiple times, we use l to refer a visit in L. For each visit $l \in L$, the charger sojourns at location x_l to recharge the sensor. After that, the charger will travel to the next sojourn location x_{l+1}.

We use y_l to denote the path between two sojourn locations x_l and x_{l+1}. Let each pair of (x_l, θ) represent a charging operation during the visit l, where the positive integer θ is an index of different charging rates. It is worth noting that the charger can decide the energy charging rates for the sensors. Increasing the charging rate will reduce the charging time for a sensor. Meanwhile, it will also spread interference over a wider area. For each visit $l \in L$, the charger can perform multiple charging operations with different energy charging rates. We therefore use $u(x_l, \theta)$ to refer the duration of charging operation (x_l, θ). During this time, a set of sensors N_l^θ will be affected by the charger's RF charging signal [13][14]. To avoid data loss, these sensors will temporarily store the data in their local storage. When the charger stops charging and moves to the next location, these sensors will be able to send out their data within such traveling duration $u(y_l, \theta)$.

Similar to the existing models [6][21], the mobile charger in our system will keep charging the WSN unless a sensor node runs out of power. The network lifetime T is therefore equal to the charger's operation time. To better balance the charging cost v_c and the network lifetime T, we apply the widely adopted utility function [16][17][21] and assume that the WSN operators can obtain profit p for each time unit when the entire network stays operational. Different from

the existing wireless charging models [20] [24], we do not assume that the energy charging rate is always higher than the network's total energy consumption rate. Our model is focusing on a more challenging scenario where the recharged energy is insufficient for the network to run forever. We will explore charing, routing as well as the profit optimization issues step-by-step in the following sections. The related notations are listed in table 1 for the sake of clarity.

4 Modeling of Charger Behaviors

In this section, we present the model of charger behaviors, including charging rates, charging interferences and charger movements.

In practice, charging rates can be dynamically adjusted by changing the power supply of the charger's RF generator. With increasing power supply, both charging rate and interference range are enlarged. Based on experimental studies [13] [14], there is roughly a proportional relationship (denote the proportional ratio as χ) between the charging rate and interference radius. Denote ϖ_{max} as the charger's maximum charging rate and R_{max} as the corresponding maximum interference radius, then we have $R_{max} = \chi\varpi_{max}$.

Next, we discuss relations between charging rates and the corresponding interfered sensor sets. Denote the distance between sensor i and the sojourn location x_l as d_{il}, for a given $l \in L$, arrange all $d_{il} < R_{max}$ $(i \in N)$ in ascending order, delete repeated distances and add R_{max} as the last element, and then we obtain a distance set $\{D_l^0, ..., D_l^{\pi_l}\}$, where π_l is the maximum number of different interfered sensor sets. And the charger can perform a maximum of π_l charging operations at lth visit [1]. In particular, we have $D_l^0 = 0$, $D_l^{\pi_l} = R_{max}$ and $D_l^{\theta-1} < D_l^{\theta}$, where the positive integer θ is an index of different interfered sensor sets (charging rates). Then, the interference radius is divided into π_l different intervals: $(D_l^0, D_l^1]$,..., $(D_l^{\pi_l-1}, D_l^{\pi_l}]$. For a given index $\theta \in [1, \pi_l]$, the interfered sensor set is defined as $N_l^{\theta} = \{i | i \in N, d_{il} < R_l^{\theta}\}$, where R_l^{θ} is the interference radius corresponds to N_l^{θ}, and we have $R_l^{\theta} \in (D_l^{\theta-1}, D_l^{\theta}]$. Actually, charging interference is unavoidable unless we can modify the sensor hardware and consider orthogonal communication channels. As shown in Fig. 2, when the charger adopts a charging rate with interference radius $R_l^2 \in (D_l^1, D_l^2]$, the interfered sensor set is $N_l^2 = \{i, j\}$.

Each pair of (x_l, θ) represent a charging operation at lth visit with index $\theta \in [1, \pi_l]$. Suppose the charger begins charging operation (x_l, θ) at time $t_l^{\theta-1}$, it keeps charging for a duration of $u(x_l, \theta)$. After that, it keeps silent (moving) for $u(y_l, \theta)$ duration until the next charging operation. Thus we have $t_l^{\theta} - t_l^{\theta-1} = u(x_l, \theta) + u(y_l, \theta)$. As shown in Fig. 3, the charger performs charging operation $(x_l, 1)$ during $[t_l^0, t_l^0 + u(x_l, 1)]$. Then, it keeps silent during $[t_l^0 + u(x_l, 1), t_l^1]$ and starts charging operation $(x_l, 2)$ at t_l^1. Note that the following properties can be easily deduced: $t_l^{\pi_l} = t_{l+1}^0$ and $t_{l+1}^0 - t_l^0 = \sum_{\theta=1}^{\theta \leq \pi_l} u(x_l, \theta) + u(y_l, \theta)$.

[1] Based on lemma 1 in section 7, if two charging operations lead to the same interfered sensor set, they can be converged to a single operation.

Table 1. List of notations.

General notations	
N	The set of sensors in the network
L	Charger's visit sequence
χ	Ratio between charging rate and interference radius
R_l^θ, R_{max}	Interference radius during $u(x_l, \theta)$ / maximum
$\varpi_l^\theta, \varpi_{max}$	Charging rate during $u(x_l, \theta)$, maximum charging rate
d_{il}	Distance between sensor i and sojourn location x_l
π_l	Maximum number of charging operations at lth visit
θ	Index of different charging rates(interfered sensor sets)
x_l	Charger's sojourn location of lth visit
y_l	Path between two sojourn locations x_l and x_{l+1}
(x_l, θ)	Charging operation at lth visit with index θ
(y_l, θ)	Intermission between two successive charging operations
D_l^θ	Interfered sensor set is N_l^θ when $R_l^\theta \in (D_l^{\theta-1}, D_l^\theta]$
N_l^θ	Interfered sensor set during $u(x_l, \theta)$
W	The charger travels W repeated paths
Φ	Approximate ratio of our near-optimal solution
ϕ^*	ϕ^* is an estimation of Φ
Profit and cost related notations	
p, P	Profit acquisition rate, the total network profit
V	The maximum investment to the sensor network
V_d, V_n, V_o	Costs during deployment, initial and operational intervals
v_f	Fixed cost to deploy the sensor network
v_d, v_c	Cost to allocate/recharge a unit of energy
Time related notations	
$t_l^{\theta-1}$	Beginning instant of charging operation (x_l, θ)
$u(x_l, \theta)$	Duration of charging operation (x_l, θ)
$u(y_l, \theta)$	Duration between two successive charging operations
T_0, T_1	End instants of initial and operational intervals
T	Network lifetime(duration of the operational interval)
t_{TL}	Time spend to visit each sensor during initial interval
τ_i	Charging duration for sensor i during initial interval
Flow routing related notations	
g_i	Data generation rate of sensor i
$g_{ij}(x_l, \theta)$	Flow routing from sensor i to sensor j during $u(x_l, \theta)$
$g_{ij}(y_l, \theta)$	Flow routing from sensor i to sensor j during $u(y_l, \theta)$
$g_i^s(x_l, \theta)$	Data storing rate for sensor i during $u(x_l, \theta)$
$g_i^r(y_l, \theta)$	Data releasing rate for sensor i during $u(y_l, \theta)$
g_{max}^r	Maximum data releasing rate
Energy related notations	
h_0	Initial battery of each sensor
h_1	Reserved energy for possible energy deficits
e	Sensor's energy consumption rate during initial interval
H_i	Battery status of sensor i at T_0
e_{il}^θ	Energy consumption of sensor i during $u(x_l, \theta)$
K_{il}^θ	Energy charged for sensor i during $u(x_l, \theta)$
$B_i(t)$	Battery status of sensor i at time t

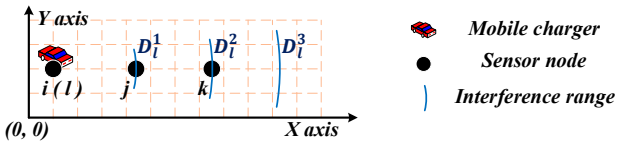

Fig. 2. The charger visits sensor i at lth visit. Here, $\pi_l = 3$ and the distance set is $\{D_l^0, D_l^1, D_l^2, D_l^3\} = \{0, d_{jl}, d_{kl}, R_{max}\}$.

Denote the charging rate of operation (x_l, θ) as ϖ_l^θ, then we have $\varpi_l^\theta = \frac{1}{\chi} R_l^\theta$. Practically, charging rates drop rapidly with increasing charging distances. As reported in [7] [14], when the charger operates with a 3 Watts ET power, sensors locate at 1 meter away acquire a charging rate of 4 mW. However, this value drops to below 0.01 mW when the distance increases to 10 meters. To ensure a high charging rate, similar to [6] [20], we assume that each sensor can be recharged only when the charger visits it. Although the charging rate is far lower than cable charging, WPT is particularly attractive since it does not require line-of-sight(LOS), and is insensitive to the neighboring environment [23]. The energy charging model in [7] can be simplified as:

$$K_{il}^\theta = \frac{1}{\chi} R_l^\theta u(x_l, \theta), \quad l \in L, \theta \in [1, \pi_l]$$

where K_{il}^θ is the energy charged for sensor i during $u(x_l, \theta)$. For sensor $j \neq i$, the charged energy is $K_{jl}^\theta = 0$.

5 Modeling of Routing Behaviors

In this section, we focus on designing a data routing that avoids data loss caused by charging interferences.

Whenever the charger recharges a sensor leveraging RF-WPT technique, data communications around it will be interfered [9] [11] [13]. For a given charging operation (x_l, θ), only if $i \notin N_l^\theta$, sensor i's data can be transmitted (or received) without loss. To avoid data loss, in this paper, we adopt a store-and-release strategy. Specifically, when sensor $i \in N_l^\theta$ suffers from interference during $u(x_l, \theta)$, it stores all to-be-transmitted data. When the charger temporarily stops charging operation during $u(y_l, \theta)$, charging interference disappears and all stored data in sensor i can be forwarded towards the sink. Take Fig. 4 as an example, when the charger performs charging operation $(x_2, 1)$, sensor 2 and 3 are interfered and their sensory data are stored. All other sensors forward data to the sink through a data routing without the participation of sensor 2 and 3. When the charger stops charging operation and moves from x_2 to x_4, sensory data can be forwarded to the sink by a routing with full sensor participation. Meanwhile, stored data in sensor 2 and 3 can be relayed towards the sink.

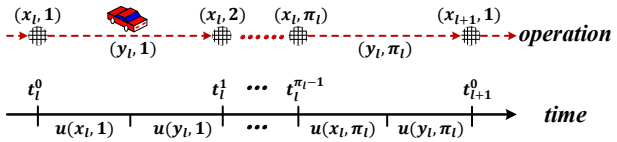

Fig. 3. Time line of charging operations.

Under this strategy, the flow routing model in [20] is extended as follows. During $u(x_l, \theta)$, we have:

$$\sum_{k \in N}^{k \neq i} g_{ki}(x_l, \theta) + g_i = \sum_{j \in N}^{j \neq i} g_{ij}(x_l, \theta) + g_{i0}(x_l, \theta) + g_i^s(x_l, \theta)$$
$$\text{For } i \in N_l^\theta : \sum_{k \in N}^{k \neq i} g_{ki}(x_l, \theta) = \sum_{j \in N}^{j \neq i} g_{ij}(x_l, \theta) = g_{i0}(x_l, \theta) = 0$$
$$\text{For } i \notin N_l^\theta : g_i^s(x_l, \theta) = 0 \tag{1}$$

where $g_{ij}(x_l, \theta)$ is the flow rate from sensor i to sensor j (subscript 0 represents the sink) and $g_i^s(x_l, \theta)$ is the data storing rate.

When the charger temporarily stops charging operation during $u(y_l, \theta)$, all stored data should be released from sensor storages and forwarded to the sink. Thus we have:

$$\sum_{k \in N}^{k \neq i} g_{ki}(y_l, \theta) + g_i = \sum_{j \in N}^{j \neq i} g_{ij}(y_l, \theta) + g_{i0}(y_l, \theta) - g_i^r(y_l, \theta) \tag{2}$$

where $g_i^r(y_l, \theta)$ is the data releasing rate from sensor i's storage. For sensor $i \notin N_l^\theta$, there is no data to be released, then $g_i^r(y_l, \theta) = 0$. As to interfered sensor $i \in N_l^\theta$, to guarantee immediate data transmission, we regulate that data stored during $u(x_l, \theta)$ must be sent out during $u(y_l, \theta)$:

$$u(x_l, \theta) g_i^s(x_l, \theta) = u(y_l, \theta) g_i^r(y_l, \theta) \tag{3}$$

However, this may cause sensors in N_l^θ release the stored data simultaneously, leading to unacceptable medium access congestions. To mitigate it, we set a maximum data releasing rate g_{max}^r and regulate that:

$$0 \leq g_i^r(y_l, \theta) \leq g_{max}^r \tag{4}$$

Although congestions can not be avoided thoroughly, decreasing data releasing rate will largely reduce the congestion possibility. The remained congestions can be mitigated by leveraging congestion resolution protocols. A detailed discussion is beyond the scope of this paper and can be found in [26].

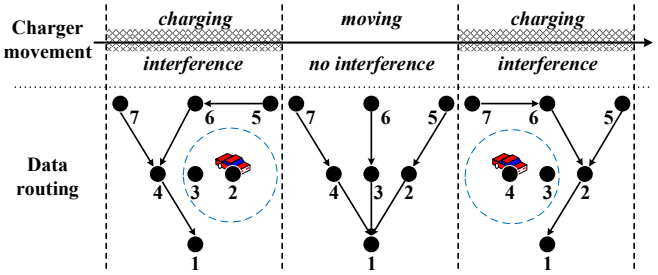

Fig. 4. An illustrative example of the proposed store-and-release strategy. The dotted circle gives the interference range, within it, data communication are prohibited to avoid possible data loss. Sensors outside the circle are unaffected. In this example, we assume that $\pi_l = 1$ holds for all $l \in L$ and the charger sojourns at x_i to visit sensor i, $i = 1, 2, .., 7$.

6 Modeling of System Profit and Cost

6.1 Deployment Interval

In typical scenarios, a sensor network's life span consists of 3 intervals: deployment, initial and operational intervals [1][27](see Fig. 5). During the first interval, sensor network is designed and sensors are deployed to the interested areas. Denote cost during deployment interval as V_d, then we have:

$$V_d = v_f + v_d N h_0$$

where v_f is the fixed cost to buy devices and to deploy the network, and v_d is the cost of a unit of energy initially allocated to sensor batteries (in contrast with wirelessly recharged energy). Note that the initial battery h_0 is an optimization variable. It will affect subsequent data routing and charger scheduling.

6.2 Initial Interval

During $[0, T_0)$, initial operations such as neighbor discovery and routing construction are performed. Let the charger visit each sensor once and recharge sensor batteries to an appropriate level to support monitoring operations during the next interval. Because the sensor network does not start collecting sensory data before T_0, interferences are not such serious in this interval. The charger is able to transfer energy at a maximum rate constantly [2], namely ϖ_{max}. Denote the charging duration for sensor i as τ_i, we have $T_0 = t_{TL} + \sum_{i \in N} \tau_i$, where t_{TL} is the charger's traveling time to visit all sensors, and the energy charged for sensor i is $\varpi_{max}\tau_i$. Denote the total costs in this interval as V_n, then we have $V_n = v_c \sum_{i \in N} \varpi_{max}\tau_i$, where v_c is the cost of a unit of recharged energy.

[2] Note that near-optimal solutions can be constructed similarly if we set energy transfer rates during this interval as variables.

Since the investment (denote as V) for the sensor network is limited, before profits are actually obtained, costs should not surpass V, namely:

$$V - V_d - V_n \geq 0 \tag{5}$$

Suppose initial operations lead to an energy consumption rate of e, and denote sensor i's battery at time T_0 as H_i, we have:

$$H_i = \varpi_{max}\tau_i + h_0 - eT_0 \geq 0, \quad i \in N \tag{6}$$

6.3 Operational Interval

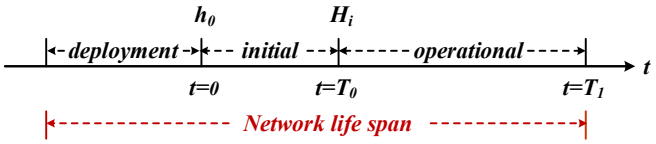

Fig. 5. Life span of a typical wireless sensor network.

After T_0, sensors begin to monitor the interested areas and profits are obtained. The duration of operational interval $[T_0, T_1]$ is defined as the network lifetime T. During $[T_0, T_1]$, sensor's energy is consumed whenever sensory data are transmitted or received. Denote $e_i(x_l, \theta)$ the energy consumption rate during $u(x_l, \theta)$ for sensor $i \in N$. In this paper, we adopt the following energy consumption model [20] [23].

$$e_i(x_l, \theta) = \sum_{k \in N}^{k \neq i} \rho g_{ki}(x_l, \theta) + \sum_{j \in N}^{j \neq i} C_{ij} g_{ij}(x_l, \theta) + C_{i0} g_{i0}(x_l, \theta)$$

where ρ is the energy consumption rate for receiving a unit of data rate and C_{ij} is the energy consumption rate for transmitting a unit of data rate from sensor i to sensor j. Specifically, $C_{ij} = \beta_1 + \beta_2 d_{ij}^{\alpha}$, where β_1 and β_2 are coefficients, and α is the path loss index. Similarly, for (y_l, θ), we have:

$$e_i(y_l, \theta) = \sum_{k \in N}^{k \neq i} \rho g_{ki}(y_l, \theta) + \sum_{j \in N}^{j \neq i} C_{ij} g_{ij}(y_l, \theta) + C_{i0} g_{i0}(y_l, \theta)$$

For sensor i, denote e_{il}^{θ} the energy consumption during $[t_l^{\theta-1}, t_l^{\theta}]$, then, we have:

$$e_{il}^{\theta} = e_i(x_l, \theta)u(x_l, \theta) + e_i(y_l, \theta)u(y_l, \theta)$$

Denote sensor i's battery status at time t as $B_i(t)$, to guarantee each sensor never run out of energy during $[T_0, T_1]$, we have:

$$B_i(t_l^{\theta}) = H_i - \sum_{\epsilon=0}^{l} \sum_{\theta=1}^{\theta \leq \pi_l} (e_{i\epsilon}^{\theta} - K_{i\epsilon}^{\theta}), \quad i \in N, l \in L \tag{7}$$

As to the cost during operational interval (denote as V_o), it is determined by the amount of recharged energy, namely:

$$V_o = v_c \sum_{l \in L} \sum_{\theta=1}^{\theta \leq \pi_l} \varpi_l^\theta u(x_l, \theta)$$

7 Joint Optimization of Charging and Routing

In this section, we formulate the joint optimization problem and show it is NP-hard. Then, we formulate a problem(UP), whose optimal solution forms an upper-bound of the original problem.

7.1 Original Problem

The network profit P is related to the network lifetime T. Since we define that the charger operates within the network during the whole network lifetime, similar to [6], the network lifetime T can be represented by the charger's operational time. Thus we have $T = \sum_{l \in L} \sum_{\theta=1}^{\theta \leq \pi_l} u(x_l, \theta) + u(y_l, \theta)$.

The joint optimization problem is formulated as:

$$\begin{aligned} \max \quad & P = Tp - V_d - V_n - V_o \\ \text{s.t.} \quad & \text{Eq. } (1) - (7) \end{aligned} \tag{OR}$$

Constraints Eq. (1) (2) are flow conservation constraints, Eq. (3) ensures that all stored data are released and forwarded to the sink, Eq. (4) regulates the maximum data release rate to mitigate medium access congestions, Eq. (5) ensures that the total cost during deployment and initial intervals will not surpass the predefined investment, Eq. (6) and Eq. (7) ensure that sensors never run out of energy during initial and operational intervals, respectively.

The original problem(OR) is highly complicated and can not be solved in polynomial time. This is because the charger's visit sequence L is determined by the charger's traveling path, and finding out an optimal traveling path is generally NP-hard. Actually, the charger's path planning sub-problem is not modeled in the above formulation. This is based on the finding that near optimal solutions can be constructed without solving this sub-problem (see section 8). Hence we can omit it here to keep the problem formulation concise.

7.2 Upper-bound Problem

Constraint Eq. (7) implies dependency between network lifetime and the charger's traveling path, which is the primary cause of the high complexity of problem (OR). To deal with it, we relax it to the following equation.

$$B_i(T_1) = H_i - \sum_{l \in L} \sum_{\theta=1}^{\theta \leq \pi_l} (e_{il}^\theta - K_{il}^\theta) \geq 0, \quad i \in N \tag{8}$$

Comparing Eq. (7) and (8), we can find that the former regulates that each sensor never run out of energy before T_1, while the latter just regulates that a sensor's total consumed energy is lesser than the total allocated/recharged energy. After relaxation, sensors are allowed to be temporarily out of power during $[T_0, T_1]$. Although the relaxation violates with the definition of network lifetime T, we will show that the out-of-power relaxation is removed by assigning extra energy h_1 to sensors in the initialization stage. Details will be presented in section 8.

Then, problem(OR) can be relaxed to problem(UP):

$$\begin{aligned} \max \quad & P = Tp - V_d - V_n - V_o \\ \text{s.t.} \quad & \text{Eq. } (1) - (6), (8) \end{aligned} \tag{UP}$$

Since the relaxed constraint Eq. (8) is a subset of Eq. (7), the optimal solution to problem(UP) forms an upper-bound of problem(OR).

7.3 Analysis of Upper-bound Problem

Before we can solve the original problem(OR), we focus on solving the relaxed problem(UP). Similar to the original problem(OR), the high complexity of problem(UP) is caused by the dependency between network lifetime and charger's traveling path. To decrease the complexity, we let the charger travel a sequential path with each sensor visited once (in arbitrary sequence), namely, $L = N$. Then, problem(UP) can be transformed to a quadratic programming problem (denote as problem(UP-N) [3]), which can be solved by CPLEX [8].

Denote the optimal solution to problem(UP-N) as S^N and the corresponding maximum profit as P^N, we give the following theorem, which says that we can obtain the optimal solution to problem(UP) by solving problem(UP-N).

Theorem 1. *S^N is the optimal solution to problem(*UP*).*

The proof of Theorem 1 is based on the following lemma.

Let $x_l = i$ represent the fact that the charger visits sensor i when it performs charging operation (x_l, θ). It is apparently that $\pi_l = \pi_i$ holds if $x_l = i$. Denote X_i^θ as the total duration in which the charger visits sensor i with an interference radius $R_l^\theta \in (D_l^{\theta-1}, D_l^\theta]$. Thus we have:

$$X_i^\theta = \sum_{l \in L}^{x_l = i} u(x_l, \theta), \quad i \in N, \theta \in [1, \pi_i]$$

Similarly, we can define

$$Y_i^\theta = \sum_{l \in L}^{x_l = i} u(y_l, \theta), \quad i \in N, \theta \in [1, \pi_i]$$

[3] Problem(UP-N) is the same as problem(UP) except for the charger's visit sequence is set to N. And problem(UP-N) is quadratic due to the quadratic term $u(x_l, \theta) g_{ij}(x_l, \theta), l \in N$.

Lemma 1. *The optimal solution to problem(*UP*) is determined by X_i^θ and Y_i^θ, and it is independent of the charger's traveling path.*

Proof. For a given $\theta \in [1, \pi_i]$ $(i \in N)$, suppose the charger performs two different operations (x_ι, θ) and (x_κ, θ) to charge the same sensor i. Namely, $\iota \neq \kappa$ and $x_\iota = x_\kappa = i$. So as to (y_ι, θ) and (y_κ, θ). To prove the above lemma, we need to prove that (x_ι, θ) and (x_κ, θ) can be converged to a single operation (x_o, θ) and the maximum profit will remain unchanged after the convergence.

Let the duration $u(x_o, \theta)$ be the sum of $u(x_\iota, \theta)$ and $u(x_\kappa, \theta)$, and other parameters of charging operation (x_o, θ) as the weighted average of (x_ι, θ) and (x_κ, θ). For example, interference radius R_o^θ and flow routing functions $g_{ij}(x_o, \theta)$ can be constructed as follows.

$$R_o^\theta = \frac{R_\iota^\theta u(x_\iota, \theta) + R_\kappa^\theta u(x_\kappa, \theta)}{u(x_o, \theta)},$$

and

$$g_{ij}(x_o, \theta) = \frac{u(x_\iota, \theta) g_{ij}(x_\iota, \theta) + u(x_\kappa, \theta) g_{ij}(x_\kappa, \theta)}{u(x_o, \theta)}$$

Next, we need to prove that all constraints of problem(*UP*) are still satisfied after the convergence.

P.1. Constraints Eq. (1) - (4) are flow routing constraints. Here we only give the proof of Eq. (1), constraints Eq. (2) - (4) can be proved in a similar way.

$$\begin{aligned}
&\sum_{k \in N}^{k \neq i} g_{ki}(x_o, \theta) + g_i \\
&= \sum_{k \in N}^{k \neq i} \frac{u(x_\iota, \theta) g_{ki}(x_\iota, \theta) + u(x_\kappa, \theta) g_{ki}(x_\kappa, \theta)}{u(x_o, \theta)} + g_i \\
&= \frac{u(x_\iota, \theta)(\sum_{k \in N}^{k \neq i} g_{ki}(x_\iota, \theta) + g_i)}{u(x_o, \theta)} + \frac{u(x_\kappa, \theta)(\sum_{k \in N}^{k \neq i} g_{ki}(x_\kappa, \theta) + g_i)}{u(x_o, \theta)} \\
&= \frac{u(x_\iota, \theta)(\sum_{j \in N}^{j \neq i} g_{ij}(x_\iota, \theta) + g_{i0}(x_\iota, \theta) + g_i^s(x_\iota, \theta))}{u(x_o, \theta)} \\
&+ \frac{u(x_\kappa, \theta)(\sum_{j \in N}^{j \neq i} g_{ij}(x_\kappa, \theta) + g_{i0}(x_\kappa, \theta) + g_i^s(x_\kappa, \theta))}{u(x_o, \theta)} \\
&= \sum_{j \in N}^{j \neq i} g_{ij}(x_o, \theta) + g_{i0}(x_o, \theta) + g_i^s(x_o, \theta)
\end{aligned}$$

P.2. Constraints Eq. (5) and (6) relate to deployment and initial intervals. Since the convergence process only relates to operational interval, Eq. (5) and (6) remains unaffected.

P.3. As to constraint Eq. (8), we need to prove that the recharged/consumed energy at (x_o, θ) is the sum of recharged/consumed energy at (x_ι, θ) and (x_κ, θ).

For the recharged energy, we have:

$$K_{io}^{\theta} = \frac{1}{\chi} R_o^{\theta} u(x_o, \theta) = \frac{1}{\chi} u(x_o, \theta) \frac{R_\iota^{\theta} u(x_\iota, \theta) + R_\kappa^{\theta} u(x_\kappa, \theta)}{u(x_o, \theta)}$$
$$= \frac{1}{\chi} R_\iota^{\theta} u(x_\iota, \theta) + \frac{1}{\chi} R_\kappa^{\theta} u(x_\kappa, \theta) = K_{i\iota}^{\theta} + K_{i\kappa}^{\theta}$$

Until now, we've proved that recharged energy is unchanged after the convergence. Similarly, we can prove that the energy consumption at (x_o, θ) equals to the sum of energy consumption at (x_ι, θ) and (x_κ, θ). Because energy recharging and consumption remain unchanged after convergence, energy constraint Eq. (8) will remain satisfied.

P.4. Finally, we analyze the optimization objective $P = Tp - V_d - V_n - V_o$. After convergence, costs V_d and V_n are unaffected, and the operational time T and cost V_o remain unchanged. Hence, the maximum network profit P will remain the same after we converge (x_ι, θ) and (x_κ, θ) together.

Based on the above illustrations, for a given visit set L, we can converge all charging operations with the same visited sensor $i \in N$ and index $\theta \in [1, \pi_i]$ to a single operation (x_i, θ). After convergence, the total duration X_i^{θ} and Y_i^{θ} remain the same, and the maximum profit P will remain unchanged. The proof of lemma 1 is concluded.

Next, we give the proof of theorem 1.

Proof. We prove theorem 1 by using contradictions. Suppose S^U is the optimal solution to problem(UP) with the maximum network profit P^U and $P^U > P^N$ holds. Based on lemma 1, we can equivalently transform problem(UP) to problem(UP-N) by converging all charging operations with the same visited sensor and index to a single operation. After convergence, the network profit will remain unchanged. Namely, we construct a solution to problem(UP-N) with network profit $P^U > P^N$, which contradicts with the fact that P^N is the maximum profit of problem(UP-N). Thus, theorem 1 is proved.

8 Solving Original Problem

In this section, we focus on constructing a near-optimal solution to the original problem(OR) and proving its approximate ratio. The relationship among problems is shown in Fig. 1 and discussed in Section I.

8.1 A Near-optimal Solution

As demonstrated by lemma 1, the maximum profit achieved by problem(UP) is independent of the charger's traveling path. Thus we can introduce an arbitrary positive integer W and let the charger travel W repeated paths. Within each

path, let each sensor be visited once (in arbitrary sequence), namely, $L = N$. The newly constructed problem can be formulated as follows:

$$\begin{aligned} \max \quad & P = W\Upsilon p - V_d - V_n - W\eta && \text{(UP-W)} \\ \text{s.t.} \quad & \frac{H_i}{W} - \sum_{l \in N} \sum_{\theta=1}^{\theta \leq \pi_l} (e_{il}^{\theta} - K_{il}^{\theta}) \geq 0, \quad i \in N && (9) \\ & L = N, \quad \text{Eq. } (1) - (6) \end{aligned}$$

Where Υ is the time duration and η is the operational cost of one of the W repeated paths. Problem(UP), (UP-N) and (UP-W) have the same optimal solution, and we can easily prove that $T = W\Upsilon$ and $V_o = W\eta$.

Actually, the optimal solution to problem(UP-W) is infeasible to the original problem(OR). This is because that the constraint Eq. (9) in problem(UP-W) is a relaxed edition of Eq. (7). Analyzing energy details of sensor i during any one of the W repeated paths, we find that the consumed energy comes from two sources: energy in sensor i's battery and energy recharged by the charger. Namely, $\frac{H_i}{W}$ and $\sum_{l \in N} \sum_{\theta=1}^{\theta \leq \pi_l} K_{il}^{\theta}$. A solution that satisfies constraint Eq. (9) may violate with Eq. (7). This is because the first source of energy ($\frac{H_i}{W}$) may be depleted before the charger visits it. Take Fig. 6(a) for example, before the charger recharges sensor i, its energy consumption surpasses $\frac{H_i}{W}$. As a result, sensor i is out of power since its battery status becomes negative.

To remove the out-of-power relaxation, we assign extra energy h_1 to each sensor. This part of energy is excluded from H_i and solely reserved for possible energy deficits. As long as h_1 is larger than the maximum possible energy consumption of each sensor during one path, constraint Eq. (7) will be satisfied. An illustrative example is shown in Fig. 6(b). We can formulate the following problem:

$$\begin{aligned} \max \quad & P = W\Upsilon p - V_d - V_i - W\eta && \text{(NR)} \\ \text{s.t.} \quad & V_d = v_d N(h_0 + h_1) && (10) \\ & h_1 = \max(\sum_{l \in N} \sum_{\theta=1}^{\theta \leq \pi_l} e_{il}^{\theta}), \quad i \in N && (11) \\ & L = N, \quad \text{Eq. } (1) - (6), (9) \end{aligned}$$

Comparing problem(NR) and (OR), we know that constraints Eq. (1) - (6) remain unchanged. As we analyzed above, Eq. (9) - (11) together ensure that constraint Eq. (7) is satisfied. Therefore, we can obtain a near-optimal solution to problem(OR) by solving problem(NR).

8.2 Approximate Ratio

Before theoretical proof of the proposed solution's approximate ratio, a simple perceptual analysis is given here. When $W \to +\infty$, the time duration $\Upsilon \to 0$.

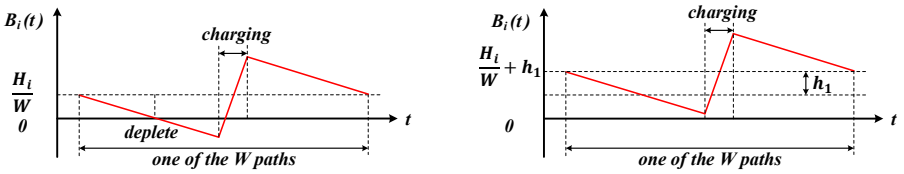

(a) Constraint Eq. (7) is violated. (b) Constraint Eq. (7) is satisfied.

Fig. 6. After relaxation, sensors are allowed to be temporarily out of power, which violates constraint Eq. (7). By assigning extra energy h_1 for each sensor, the out-of-power relaxation is removed. Hence, the optimal solution to problem(NR) is a feasible solution to the original problem(OR).

Then, $h_1 \to 0$ and problem(NR) will become infinite close to problem(UP-W). Since problem(UP-W) forms an upper-bound of the original problem, our near-optimal solution can reach a very high approximate ratio if $W \to +\infty$.

Since the approximate ratio is hard to determine directly, we construct a virtual problem(LOW) (actually, problem(LOW) is nonexistent, we use (LOW) for description simplicity), whose optimal solution forms a lower-bound of problem (NR). And we let the ratio between problem(LOW) and (UP) to represent the desired approximate ratio. The following steps can be deemed as the solving processes to problem(LOW).

S.1. Denote optimal solutions to problem (UP-W) and (LOW) as $\overline{S}$ and S^*, respectively. For discrimination simplicity, we mark all constitutes of solution $\overline{S}$ with bars, and those of S^* with stars. For example, the maximum profit achieved by solution $\overline{S}$ is $\overline{P}$, and that achieved by S^* is P^*. We introduce a variable $\phi \in (0, 1]$ and let $u^*(x_l, \theta) = \phi\overline{u}(x_l, \theta)$ and $u^*(y_l, \theta) = \phi\overline{u}(y_l, \theta)$.

S.2. We construct the following optimization problem to obtain constituents of S^* during deployment and initial intervals.

$$\begin{aligned} \max \quad & \phi \\ \text{s.t.} \quad & H_i = \phi\overline{H}_i \\ & \text{Eq. } (5), (6), (10), (11) \end{aligned} \tag{EN}$$

Note that variables in problem(EN) are h_0, h_1, V_d, τ_i, T_0, V_i, H_i and ϕ.

S.3. Except for constituents calculated from **S.2**, we let S^* copy all other constituents from solution $\overline{S}$.

We give the following theorem, which says that S^* is a lower-bound of problem(NR).

Theorem 2. *S^* is a solution to problem(*NR*) with profit $P^* = \phi^* W\overline{\Upsilon}p - V_d^* - V_n^* - \phi^* W\overline{\eta}$, where ϕ^*, V_d^*, V_n^* are obtained by solving problem(*EN*).*

Proof. First, we need to prove S^* is a feasible solution to problem(NR). Since constituents of S^* during deployment and initial intervals are obtained by solving problem(EN), constraint Eq. (5), (6), (10), (11) are satisfied. Constraints Eq.

(1) - (4) are also satisfied because S^* copies flow routings from $\overline{S}$. Then, we emphasize on the constraint Eq. (9). We can easily prove that $e_{il}^{*\theta} = \phi^* \overline{e}_{il}^{\theta}$ and $K_{il}^{*\theta} = \phi^* \overline{K}_{il}^{\theta}$, thus we have:

$$\begin{aligned}\frac{H_i^*}{W} - \sum_{l \in N} \sum_{\theta=1}^{\theta \leq \pi_l} (e_{il}^{*\theta} - K_{il}^{*\theta}) &= \frac{\phi^* \overline{H}_i}{W} - \sum_{l \in N} \sum_{\theta=1}^{\theta \leq \pi_l} (\phi^* \overline{e}_{il}^{\theta} - \phi^* \overline{K}_{il}^{\theta}) \\ &= \phi^* [\frac{\overline{H}_i}{W} - \sum_{l \in N} \sum_{\theta=1}^{\theta \leq \pi_l} (\overline{e}_{il}^{\theta} - \overline{K}_{il}^{\theta})] \geq 0\end{aligned}$$

Because all constraints of problem(NR) are satisfied by solution S^*, it is a feasible solution to problem(NR). Thus S^* forms a lower-bound of the optimal solution to problem(NR). We can easily prove that $\Upsilon^* = \phi^* \overline{\Upsilon}$ and $\eta^* = \phi^* \overline{\eta}$, thus we have $P^* = \phi^*\ W\overline{\Upsilon}p\ -V_d^*\ -V_i^*\ -\phi^* W\overline{\eta}$.

The approximate ratio Φ can be calculated by:

$$\Phi = \frac{P^*}{\overline{P}} = \frac{\phi^* W\overline{\Upsilon}p - V_d^* - V_i^* - \phi^* W\overline{\eta}}{W\overline{\Upsilon}p - \overline{V}_d - \overline{V}_i - W\overline{\eta}} = \frac{\phi^* - \frac{1}{W(\overline{\Upsilon}p - \overline{\eta})}(V_d^* + V_i^*)}{1 - \frac{1}{W(\overline{\Upsilon}p - \overline{\eta})}(\overline{V}_d + \overline{V}_i)} \approx \phi^*$$

Because $W(\overline{\Upsilon}p - \overline{\eta})$ is much larger than both $V_d^* + V_i^*$ and $\overline{\Upsilon}p - \overline{\eta}$, ϕ^* can be recognized as an estimation of Φ.

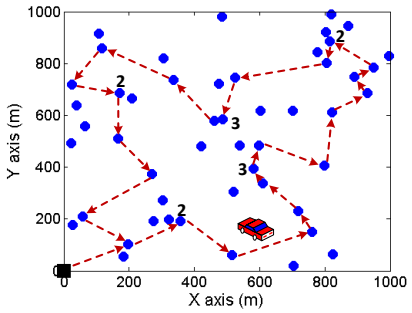

Fig. 7. The charger's traveling path for a randomly generated 50-sensor network. The number marked near a sensor represents that multiple charging operations are performed.

9 Evaluation

In this section, we evaluate our solution under different parameter settings and give comparisons to show its effectiveness.

9.1 Simulation Setup

We assume that a number of sensors are randomly distributed over a 1 km $\times$ 1 km two-dimensional square area, the sink is located at (0, 0), and each sensor's data generation rate is randomly generated within $[1, 10]$ kb/s. Energy consumption coefficients $\beta_1 = 5$ nJ/b, $\beta_2 = 1.3 \times 10^{-4}$ pJ/(b$\cdot m^4$), $\alpha = 4$ and $\rho = 5$ nJ/b [20] [24]. The charger sojourns at the sink when $t = 0$. The maximum interference radius is $R_{max} = 150$ m and the proportional ratio between interference and energy transfer rate is $\chi = 1000$ (m $\cdot$ s)/J, leading to the maximum energy transfer rate $\varpi_{max} = 0.15$ J/s.

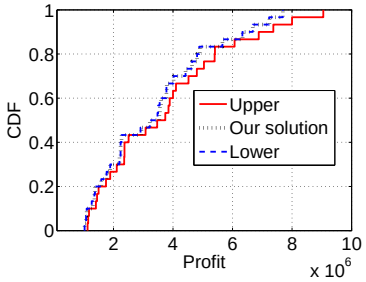

Fig. 8. Profits of 100 runs.

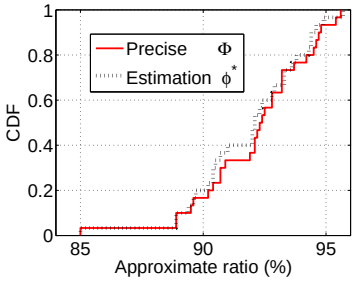

Fig. 9. Optimality of 100 runs.

We set the total investment and fixed cost to be proportional to the total number of sensors. Namely, $V = 1000 \cdot N$ and $v_f = 0.1 \cdot V$. The cost of a unit of allocated energy is $v_d = 0.1\ J^{-1}$ while the cost to charge a unit of energy wirelessly is $v_c = 0.2\ J^{-1}$. Whenever the interested area is monitored successfully for a unit of time, $p = 10$ profit is acquired. The energy consumption rate during initial interval is $e = 1 \times 10^{-4}$ J/s. Moreover, the maximum data releasing rate is $g^r_{max} = 10$ kb/s, and the charger's traveling time is $t_{TL} = 1000$ s.

9.2 Approximate Ratio

In this part, we focus on the approximate ratio of our solution. We run the simulation 100 times with different random seeds, network scale (20 to 100 sensors) and sensor deployments. Results are presented in Fig. 8 and 9. Under varied network environments, our solution achieves [85%, 95.6%] approximate ratio, with an average value of 92.1%. The estimated approximate ratio ϕ^* is very accurate and the deviation is varied between [-3.25%, 0.11%], with an average value of -0.26%.

9.3 Baseline Setup

Currently, there is no existing work that jointly considers charger scheduling and data routing under the practical charging interference concern. Some similar

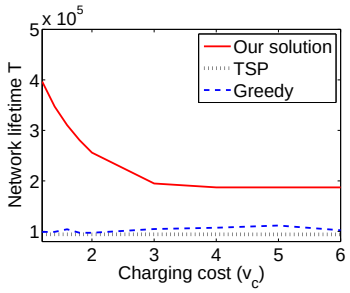

Fig. 10. Network lifetime.

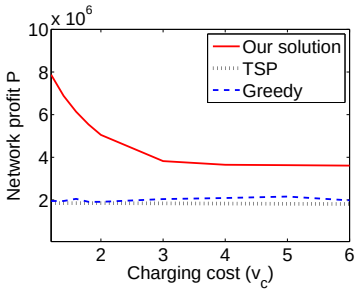

Fig. 11. Profit.

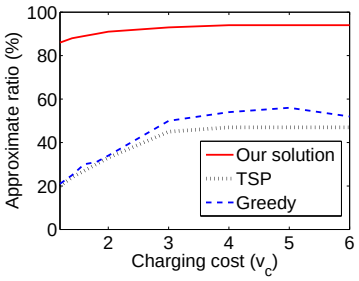

Fig. 12. Approximate ratio.

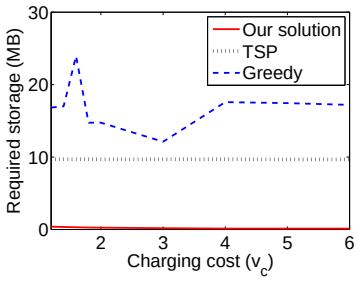

Fig. 13. Required Storage.

works predefine the charger's traveling path to TSP to decrease the complexity of the joint optimization problems [20] [24]. To compare the performance of our solution, we introduce a baseline setup that also regulates the charger's path to a TSP. In terms of energy allocation, the baseline adopts the pervasively used method which averagely allocates as much energy as possible to each sensor during deployment interval.

Another group of studies borrow the concept of greedy searching, where the charger always first visits the sensor of the most urgent energy requirement [6]. We construct our second baseline based on the greedy idea. Note that the proposed store-and-release strategy is incorporated in both baseline designs to avoid data loss and to ensure that the comparisons are in the fair positions.

9.4 Performance Comparisons

The system performance of various designs are comprehensively examined in the following aspects: network lifetime, profit, approximate ratio and required storage. Since the charging cost v_c has significant impacts on system performances, each aspect is investigated under varied values of v_c. Although other system parameters such as V, v_d and g^r_{max} also exhibit impacts on the system performance, they are omitted due to limited space.

Network Lifetime As shown in Fig. 11, v_c affects different designs in different ways. The maximum network lifetime achieved by our solution decreases with the increasing charging cost v_c. When v_c is small, our solution achieves above 300% lifetime gains compared to TSP and greedy baselines. Even with the increasing cost, above 67.6% lifetime gains can be easily observed. In terms of TSP baseline, v_c shows little impact. This is because the original joint optimization problem is largely simplified after we regulate the charger's traveling path to TSP. And data routing becomes the most important optimization variable, which shows gentler effect on system performances. The greedy baseline exhibits slight randomness when v_c increases. The increasing v_c affects charging operation durations, thus affects sensor's energy consumption. Following the greedy idea, the charger's traveling path is uncertain, leading to randomness of the final network lifetime.

Network Profit As discussed in [16] [17] [21], the optimization objective of maximizing network profit P achieves better balance between network lifetime T and charging costs. As shown in Fig. 10 and 11, T and P exhibit similar regularities, which validates that P is a good indicator of T. The larger profit achieved by our solution is based on prolonged network lifetime. Compared with TSP and greedy baselines, the profit gains achieved by our solution varies between [99.5%, 325.4%] and [68.1%, 303.6%], respectively.

Approximate Ratio In this part, the approximate ratio is defined as the ratio between a design and the upper-bound profit $\overline{P}$. From Fig. 12, we can see [86%, 94%] approximate ratio of our solution, which validates its high performance. Approximate ratios of TSP and greedy baselines vary between [20%, 47%] and [21%, 56%], respectively.

Required Storage Since all designs adopt the proposed store-and-release strategy, additional storages are required to store sensory data when a sensor is interfered by the charger. As shown in Fig. 13, our solution requires a very small additional storage. As v_c increases, the required storage decreases from 0.38 MB to 0.12 MB. Such a small amount of additional storage can be easily satisfied even in resource limited sensors. Contrarily, the TSP baseline constantly requires about 9.7 MB storage and the greedy baseline requires a larger storage varying from 12.1 MB to 23.9 MB.

In summary, our solution achieves high approximate ratio in different network environments. Compared to the widely used concepts such as TSP path and greedy searching, our solution obtains up to 300% higher network lifetime.

10 Conclusion

In this paper, we have investigated the joint optimization problem under the practical charging interference consumptions. Based on the proposed constraint relaxation techniques, we have constructed a near-optimal solution of the joint

optimization problem. The effectiveness of our solution is validated with extensive simulations and comparisons. In our future work, we will further explore the situation with very large scale sensor networks and multiple wireless chargers. And we also plan to incorporate duty cycling methods with mobile chargers to further prolong the sensor network lifetime.

References

1. G. Anastasi, M. Conti, M. Di Francesco, and A. Passarella. Energy conservation in wireless sensor networks: A survey. *Elsevier Ad Hoc networks*, 7(3):537–568, 2009.
2. S. Bandyopadhyay and E. J. Coyle. An energy efficient hierarchical clustering algorithm for wireless sensor networks. In *IEEE INFOCOM*, volume 3, pages 1713–1723, 2003.
3. H. Dai, Y. Liu, G. Chen, X. Wu, and T. He. Safe charging for wireless power transfer. In *IEEE INFOCOM*, pages 1105–1113, 2014.
4. L. Fu, P. Cheng, Y. Gu, J. Chen, and T. He. Minimizing charging delay in wireless rechargeable sensor networks. In *IEEE INFOCOM*, pages 2922–2930, 2013.
5. K. Gudan, S. Chemishkian, J. J. Hull, M. S. Reynolds, and S. Thomas. Feasibility of wireless sensors using ambient 2.4 GHz RF energy. In *IEEE Sensors*. Citeseer, 2012.
6. S. Guo, C. Wang, and Y. Yang. Mobile data gathering with wireless energy replenishment in rechargeable sensor networks. In *IEEE INFOCOM*, pages 1932–1940, 2013.
7. S. He, J. Chen, F. Jiang, D. K. Yau, G. Xing, and Y. Sun. Energy provisioning in wireless rechargeable sensor networks. *IEEE Trans. Mobile Computing*, 12(10):1931–1942, 2013.
8. IBM CPLEX Optimizer. http://www-01.ibm.com/software/integration/optimization/cplex-optimizer/.
9. B. Kellogg, A. Parks, S. Gollakota, J. R. Smith, and D. Wetherall. Wi-fi backscatter: internet connectivity for rf-powered devices. In *ACM SIGCOMM*, pages 607–618, 2014.
10. A. Kurs, A. Karalis, R. Moffatt, J. D. Joannopoulos, P. Fisher, and M. Soljačić. Wireless power transfer via strongly coupled magnetic resonances. *Science*, 317(5834):83–86, 2007.
11. V. Liu, A. Parks, V. Talla, S. Gollakota, D. Wetherall, and J. R. Smith. Ambient backscatter: wireless communication out of thin air. In *ACM SIGCOMM*, pages 39–50, 2013.
12. J. Luo and J.-P. Hubaux. Joint mobility and routing for lifetime elongation in wireless sensor networks. In *IEEE INFOCOM*, volume 3, pages 1735–1746, 2005.
13. M. Y. Naderi, K. R. Chowdhury, S. Basagni, W. Heinzelman, S. De, and S. Jana. Experimental study of concurrent data and wireless energy transfer for sensor networks. In *IEEE GLOBECOM*, 2014.
14. M. Y. Naderi, K. R. Chowdhury, S. Basagni, W. Heinzelman, S. De, and S. Jana. Surviving Wireless Energy Interference in RF-harvesting Sensor Networks: An Empirical Study. In *IEEE SECON*, 2014.
15. A. N. Parks, A. Liu, S. Gollakota, and J. R. Smith. Turbocharging ambient backscatter communication. In *ACM SIGCOMM*, pages 619–630, 2014.
16. T. L. Porta, C. Petrioli, C. Phillips, and D. Spenza. Sensor mission assignment in rechargeable wireless sensor networks. *ACM TOSN*, 10(4):60, 2014.

17. T. L. Porta, C. Petrioli, and D. Spenza. Sensor-mission assignment in wireless sensor networks with energy harvesting. In *IEEE SECON*, pages 413–421, 2011.
18. Y. Qu, K. Xu, J. Liu, and W. Chen. Towards a practical energy conservation mechanism with assistance of resourceful mules. *IEEE Internet of Things Journal*, 2(2):145–158, 2015.
19. A. P. Sample, D. J. Yeager, P. S. Powledge, A. V. Mamishev, and J. R. Smith. Design of an rfid-based battery-free programmable sensing platform. *IEEE Trans. Instrumentation and Measurement*, 57(11):2608–2615, 2008.
20. Y. Shi, L. Xie, Y. T. Hou, and H. D. Sherali. On renewable sensor networks with wireless energy transfer. In *IEEE INFOCOM*, pages 1350–1358, 2011.
21. C. Wang, J. Li, F. Ye, and Y. Yang. Recharging schedules for wireless sensor networks with vehicle movement costs and capacity constraints. In *IEEE SECON*, pages 468–476, 2014.
22. L. Xie, Y. Shi, Y. T. Hou, and A. Lou. Wireless power transfer and applications to sensor networks. *IEEE Wireless Communications Magazine*, 20(4), 2013.
23. L. Xie, Y. Shi, Y. T. Hou, W. Lou, H. Sherali, and S. F. Midkiff. Multi-node wireless energy charging in sensor networks. *IEEE Trans. on Networking (accepted)*, 2015.
24. L. Xie, Y. Shi, Y. T. Hou, W. Lou, H. D. Sherali, and S. F. Midkiff. Bundling mobile base station and wireless energy transfer: Modeling and optimization. In *IEEE INFOCOM*, pages 1636–1644, 2013.
25. Y. Xu, J. Heidemann, and D. Estrin. Geography-informed energy conservation for Ad Hoc routing. In *ACM MOBICOM*, pages 70–84, 2001.
26. W. Ye, J. Heidemann, and D. Estrin. An energy-efficient MAC protocol for wireless sensor networks. In *IEEE INFOCOM*, volume 3, pages 1567–1576, 2002.
27. J. Yick, B. Mukherjee, and D. Ghosal. Wireless sensor network survey. *Elsevier Computer networks*, 52(12):2292–2330, 2008.
28. S. Zhang, Z. Qian, F. Kong, J. Wu, and S. Lu. P3: Joint optimization of charger placement and power allocation for wireless power transfer. In *IEEE INFOCOM*, 2015.
29. W. Zhao, M. Ammar, and E. Zegura. A message ferrying approach for data delivery in sparse mobile Ad Hoc networks. In *ACM MOBIHOC*, pages 187–198, 2004.